The TSIS-1 Hybrid Solar Reference Spectrum

Odele M Coddington[1], Erik C Richard[2], Dave Harber[2], Peter Pilewkie[3], Thomas N. Woods[4], Kelly V. Chance[5], Xiong Liu[5], and Kang Sun[6]

[1]University of Colorado Boulder, LASP
[2]University of Colorado, LASP
[3]University of Colorado Boulder
[4]Laboratory for Atmospheric and Space Physics
[5]Harvard-Smithsonian Center for Astrophysics
[6]University at Buffalo, State University of New York

November 30, 2022

Abstract

We present a new solar irradiance reference spectrum representative of solar minimum conditions between solar cycles 24 and 25. The Total and Spectral Solar Irradiance Sensor-1 (TSIS-1) Hybrid Solar Reference Spectrum (HSRS) is developed by applying a modified spectral ratio method to normalize very high spectral resolution solar line data to the absolute irradiance scale of the TSIS-1 Spectral Irradiance Monitor (SIM) and the CubeSat Compact SIM (CSIM). The high spectral resolution solar line data are the Air Force Geophysical Laboratory ultraviolet solar irradiance balloon observations, the ground-based Quality Assurance of Spectral Ultraviolet Measurements In Europe Fourier transform spectrometer solar irradiance observations, the Kitt Peak National Observatory solar transmittance atlas, and the semi-empirical Solar Pseudo-Transmittance Spectrum atlas. The TSIS-1 HSRS spans 202 nm to 2730 nm at 0.01 to ~0.001 nm spectral resolution with uncertainties of 0.3% between 400 and 2365 nm and 1.3% at wavelengths outside that range.

The TSIS-1 Hybrid Solar Reference Spectrum

O. M. Coddington[1], E. C. Richard[1], D. Harber[1], P. Pilewskie[1,2], T. N. Woods[1], K. Chance[3], X. Liu[3], and K. Sun[4,5]

[1]Laboratory for Atmospheric and Space Physics, University of Colorado Boulder, USA.

[2]Department for Atmospheric and Oceanic Science, University of Colorado Boulder, USA.

[3] Harvard-Smithsonian Center for Astrophysics, Cambridge, USA.

[4] Department of Civil, Structural and Environmental Engineering, University at Buffalo, Buffalo, USA.

[5] Research and Education in eNergy, Environment and Water (RENEW) Institute, University at Buffalo, Buffalo, USA.

Corresponding author: Odele Coddington (odele.coddington@lasp.colorado.edu)

†Additional author notes should be indicated with symbols (current addresses, for example).

Key Points:

- The TSIS-1 Spectral Irradiance Monitor and Compact SIM instruments observe the Sun's irradiance spectrum at high accuracy.
- The TSIS-1 Hybrid Solar Reference Spectrum consists of high resolution solar line data normalized to the TSIS-1 SIM irradiance spectrum.
- The TSIS-1 Hybrid Solar Reference Spectrum has at least 0.01 nm spectral resolution, spans 202 to 2730 nm, and is accurate to 0.3 to 1.3%.

Abstract

We present a new solar irradiance reference spectrum representative of solar minimum conditions between solar cycles 24 and 25. The Total and Spectral Solar Irradiance Sensor-1 (TSIS-1) Hybrid Solar Reference Spectrum (HSRS) is developed by applying a modified spectral ratio method to normalize very high spectral resolution solar line data to the absolute irradiance scale of the TSIS-1 Spectral Irradiance Monitor (SIM) and the CubeSat Compact SIM (CSIM). The high spectral resolution solar line data are the Air Force Geophysical Laboratory ultraviolet solar irradiance balloon observations, the ground-based Quality Assurance of Spectral Ultraviolet Measurements In Europe Fourier transform spectrometer solar irradiance observations, the Kitt Peak National Observatory solar transmittance atlas, and the semi-empirical Solar Pseudo-Transmittance Spectrum atlas. The TSIS-1 HSRS spans 202 nm to 2730 nm at 0.01 to ~0.001 nm spectral resolution with uncertainties of 0.3% between 400 and 2365 nm and 1.3% at wavelengths outside that range.

Plain Language Summary

The Sun's irradiance spectrum is used in many applications, such as constraining the solar forcing in climate models and converting measured satellite radiance to reflectance. A growing body of literature has provided evidence that the currently available solar reference spectra differ by more than their reported uncertainties. Such differences lead to biased results when different reference spectra are adopted in the aforementioned applications. This motivates our work to provide a new high-resolution solar reference spectrum at higher accuracy than any previously reported. Our ability to produce such a dataset is due to the state-of-the-art measurements of the Sun's irradiance spectrum made since March 2018 by the next-generation Spectral Irradiance Monitor (SIM) instrument on the Total and Spectral Solar Irradiance Sensor-1 (TSIS-1) satellite mission and the Compact SIM (CSIM) technology demonstration mission. The TSIS-1 SIM and CSIM have order-of-magnitude reduction in uncertainty relative to predecessor instruments primarily because of a first-of-its-kind spectral radiometric calibration facility capable of characterizing the instruments to higher fidelity. We develop this new, high-resolution, solar irradiance reference spectrum by adjusting high spectral resolution solar line data to the irradiance scale of the more accurate, but lower spectral resolution, TSIS-1 SIM and CSIM observations.

1 Introduction

Reference solar irradiance spectra have broad utility in atmospheric science and climate applications. For example, the incoming solar spectral irradiance is used to convert measured satellite radiance to reflectance (e.g., Wielicki et al., 2013) and as the upper boundary condition in radiative transfer models used, for example, in remote sensing algorithms and renewable energy research (e.g., Berk et al., 2014; Apell & McNeill, 2019). Some instruments use the absorption lines in a reference spectrum for wavelength calibration (e.g., Kang et al., 2020). Some instruments also use the Sun as a radiometric calibration source for stability monitoring, which first requires a solar reference spectrum as a baseline against which to quantify instrumental changes (e.g., Pan & Flynn, 2015). Instruments that assess the stability of their radiometric calibration relative to the moon (e.g., Werdell et al., 2019) indirectly rely on a solar reference spectrum to convert lunar radiance to reflectance using, for example, the RObotic Lunar Observatory (ROLO) model (Kieffer & Stone, 2005). Solar reference spectra are also used to constrain solar irradiance variability models (e.g., Coddington et al. 2016) which climate models use to specify solar forcing of climate change (e.g., Kunze et al., 2020).

A number of existing solar reference spectra are available for the applications listed above. Some are from direct observations of the Sun's irradiance from one or more satellite instruments. These have relatively high reported accuracy and relatively low (0.1 nm or poorer) spectral resolution compared to ground-based observations and are typically specific to certain solar activity levels (e.g., Thuillier et al., 2004; Woods et al., 2009; Meftah et al., 2020). Other solar reference spectra are constructed by normalizing high spectral resolution solar lines to a high accuracy, low spectral resolution, irradiance spectrum (e.g., Chance and Kurucz, 2010). Still other reference spectra are created by concatenating independent datasets from different spectral regions (e.g., Gueymard, 2003). Such approaches are necessary because the technology does not exist to measure the Sun's spectrum over a broad spectral range from a single instrument with both high accuracy and high (0.01 nm or finer) spectral resolution. A growing body of literature has identified disagreements between the available solar reference spectra irradiance scales with independent measurements that often exceed the quoted accuracies, particularly at near-infrared wavelengths where differences reaching 8% have been reported (e.g., Elsey et al., 2017).

Since March 2018, NASA's Total and Spectral Solar Irradiance Sensor-1 (TSIS-1) Spectral Irradiance Monitor (SIM) hosted on the International Space Station has observed solar spectral irradiance with lower radiometric uncertainty (< 0.3%) over the majority of the spectrum than that attained by any previous instrument (Richard et al., 2020). Since 2019, independent observations of solar spectral irradiance measurements have also been made by the Compact SIM (CSIM) instrument from a CubeSat technology demonstration mission (Richard et al., 2019; Tomlin et al., 2020). CSIM observations span 200 nm to 2800 nm, thereby extending further into the infrared than the TSIS-1 SIM that spans 200 nm to 2400 nm. A mutual validation of the TSIS-1 SIM and CSIM irradiance scales was demonstrated by less than 1% disagreement in concurrent observations (Stephens et al., 2020).

Figure 1 shows the spectral difference of three established solar irradiance reference spectra to TSIS-1 SIM with disagreements reaching or exceeding 10%, particularly in the ultraviolet and near-infrared portions of the spectrum. The ATLAS-3 spectrum (Thuillier et al., 2004), perhaps the most widely-used solar reference in Earth science applications, is a composite of solar observations from November, 1994 by five different instruments on two different platforms: the Upper Atmospheric Research Satellite and the ATLAS shuttle mission. Additionally, high resolution modeled solar absorption features from Kurucz (1995) were inserted into the lower resolution observations from the visible through the near-infrared. Reported ATLAS-3 uncertainties are 2-3%. Another frequently used solar reference spectrum is the Laboratory for Atmospheric and Space Physics (LASP) Whole Heliospheric Interval (WHI) (Woods et al., 2009). The LASP WHI is a composite of solar observations with the majority of the spectrum measured during April, 2008 by two instruments on the Solar Radiation and Climate Experiment (SORCE) satellite, SOLSTICE and SIM. The observations from SORCE SIM, the predecessor to the TSIS-1 SIM, were adjusted upwards by as much as 8% for wavelengths above 1350 nm to agree with the ATLAS-3 spectrum in a recalibration that has been discussed with reference to a systematic bias (Harder et al., 2010). Therefore, the LASP WHI and ATLAS-3 reference spectra are not independent above 1350 nm. Reported LASP WHI uncertainties are 1-3% for wavelengths above 300 nm. Yet another solar reference spectrum is

SOLAR-ISS version 2 (Meftah et al., 2020). SOLAR-ISS is from a newer version of the SOLar SPECtrometer (SOLSPEC) than what was flown during the ATLAS era. The SOLAR-ISS reference irradiance baseline spectrum is from April, 2008 for wavelengths spanning 165-656 nm and an average over a six year period at wavelengths above 656 nm. Revised engineering corrections, improved calibrations, and advanced thermal and degradation corrections are reported as the reason for the changes in the baseline between the earlier ATLAS-3 and the newer SOLAR-ISS spectra. Similar to the ATLAS-3 approach, higher spectral resolution lines have been incorporated into SOLAR-ISS. The mean reported SOLAR-ISS uncertainty from 165 to 3000 nm is 1.26%, with uncertainties as low as 0.4-0.6% between 800 to 1700 nm and reaching, or exceeding, 2% below 400 nm and above 2200 nm. Hilbig et al. (2018) summarize the characteristics of other solar reference spectra than those discussed here.

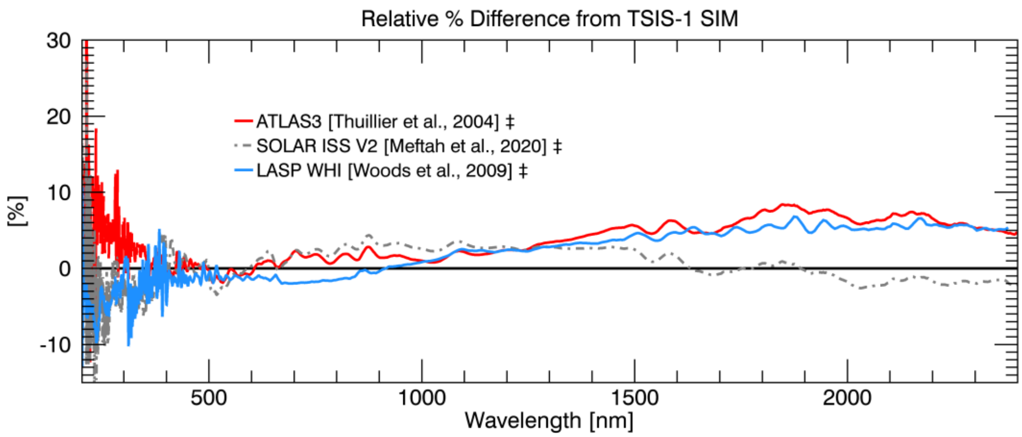

Figure 1. Percent relative difference between the ATLAS-3, SOLAR-ISS (v2) and LASP WHI solar reference spectra from TSIS-1 SIM. All datasets have been convolved to the TSIS-1 SIM spectral resolution prior to computing the difference as (Reference – TSIS-1 SIM) / TSIS-1 SIM x 100.

The results shown in Figure 1 motivate our work to produce a new solar reference spectrum, the *TSIS-1 Hybrid Solar Reference Spectrum* (*TSIS-1 HSRS*), by adjusting high spectral resolution solar line data to the absolute, SI-traceable, irradiance scale of the more accurate, but lower spectral resolution, TSIS-1 SIM and CSIM observations. The methodology to develop the HSRS is described in Section 2 and the datasets are described in Section 3. In Section 4, we present our results, describe our uncertainty assessment, and compare the HSRS to independent datasets. Concluding statements follow in Section 5.

2 Methodology

We apply a modified version of the spectral ratio method to develop the HSRS. In this method, a wavelength-dependent scaling factor adjusts high spectral resolution datasets ($\boldsymbol{\beta}$) to match a lower resolution but higher accuracy spectrum ($\boldsymbol{\alpha}$). The scaling factor, Q, is derived from the ratio of the $\boldsymbol{\alpha}$ and $\boldsymbol{\beta}$ datasets after first convolving both to the same spectral resolution and interpolating to a common sampling grid. The $\boldsymbol{\alpha}$ and $\boldsymbol{\beta}$ datasets are described in Section 3.

Typically, the Q factor is derived after a single-step convolution (Eq. 1) of the $\boldsymbol{\beta}$ dataset with the instrument line shape of the $\boldsymbol{\alpha}$ dataset ($\boldsymbol{ILS_{\alpha}}$) that degrades the resolution of the $\boldsymbol{\beta}$

dataset ($\boldsymbol{\beta}^{*}$) to match that of the $\boldsymbol{\alpha}$ dataset (e.g., Kang et al., 2017; Dobber et al., 2008). In our modification, we apply a two-step convolution in deriving our *Q* factor: the first step is as described by Eq. 1 and the second step degrades both $\boldsymbol{\beta}^{*}$ and $\boldsymbol{\alpha}$ datasets to a common spectral resolution (denoted $\boldsymbol{\beta}^{**}$ and $\boldsymbol{\alpha}^{**}$, respectively) that is coarser than that of the original $\boldsymbol{\alpha}$ dataset. We accomplish this by convolution with a Gaussian filter ($\mathbb{N}$) of specified standard deviation ($\boldsymbol{\sigma}$) (Eq. 2). The two-step convolution reduces the impacts of any uncertainty in $\boldsymbol{ILS_{\alpha}}$ on the *Q* factor defined in Eq. 3, where the subscript ‡ denotes an interpolation of the $\boldsymbol{\beta}^{**}$ dataset to the $\boldsymbol{\alpha}^{**}$ sampling grid. Finally, the adjusted $\boldsymbol{\beta}$ dataset (denoted by $\boldsymbol{\Upsilon}$) is computed from the product of the native $\boldsymbol{\beta}$ dataset and the *Q* factor, where the subscript † denotes an interpolation of the *Q* factor to the native $\boldsymbol{\beta}$ sampling grid (Eq. 4).

$$\boldsymbol{\beta}^{*} = \boldsymbol{\beta} \otimes \boldsymbol{ILS_{\alpha}} \tag{1}$$

$$\boldsymbol{\beta}^{**} = \boldsymbol{\beta}^{*} \otimes \mathbb{N}(\boldsymbol{\sigma}) \textbf{ and } \boldsymbol{\alpha}^{**} = \boldsymbol{\alpha} \otimes \mathbb{N}(\boldsymbol{\sigma}) \tag{2}$$

$$\boldsymbol{Q} = \boldsymbol{\alpha}^{**}/\boldsymbol{\beta}^{**}_{\ddagger} \tag{3}$$

$$\boldsymbol{\Upsilon} = \boldsymbol{\beta} \times \boldsymbol{Q}_{\dagger} \tag{4}$$

$\boldsymbol{\Upsilon}$ represents the $\boldsymbol{\beta}$ datasets at the absolute irradiance scale of the $\boldsymbol{\alpha}$ spectrum. $\boldsymbol{\Upsilon}$ datasets differ from the native $\boldsymbol{\beta}$ datasets in their broad baseline features, but share the same native spectral and sampling resolutions. The TSIS-1 HSRS is the concatenation of these $\boldsymbol{\Upsilon}$ datasets. In transition regions, where one $\boldsymbol{\Upsilon}$ dataset overlaps in wavelength with another, we adopt an average of the irradiance values for the HSRS.

3 Data

3.1 High Accuracy ($\boldsymbol{\alpha}$) Spectrum

Our high accuracy $\boldsymbol{\alpha}$ spectrum is from TSIS-1 Spectral Irradiance Monitor (SIM) and Compact SIM (CSIM) space-based observations of solar spectral irradiance. TSIS-1 SIM has measured daily spectral irradiance between 200-2400 nm since March 2018. The CSIM dataset, spanning 210-2800 nm, began in late-March 2019. The SIM instruments are prism spectrometers with variable spectral resolution of approximately 0.25 to 40 nm (Richard et al., 2019; 2020). TSIS-1 SIM and CSIM data are available from these websites: https://lasp.colorado.edu/home/tsis/data/ssi-data/ and https://lasp.colorado.edu/home/csim/data-and-ham-radio/.

TSIS-1 SIM has order-of-magnitude reductions in radiometric uncertainty relative to the heritage SORCE SIM instrument (Harder et al., 2005) through an extensive component level calibration program that characterized the instrument as an absolute sensor and verified the instrument in irradiance across the spectrum against an SI-traceable cryogenic radiometer using stable tunable laser sources (Richard et al. 2020). The instrument level validation and final end-to-end absolute calibration placed relative pre-launch accuracy uncertainties at 0.24% (>400 nm) to 0.41% (<400 nm). On-orbit calibration stability is maintained by instrument degradation corrections that utilize observations made by redundant and independent instrument channels that are exposed to the Sun at varying duty cycles (Mauceri et al., 2020).

CSIM is a 6U CubeSat technology demonstration mission for the NASA Earth Science Technology Office In-Space Validation of Earth Science Technologies program. CSIM radiometric accuracy is tied to the same SI-traceable cryogenic radiometer with the same laser sources used in the TSIS-1 SIM calibrations, but by calibration transfer as opposed to absolute calibration verification. Based on this calibration, the CSIM measurement uncertainty is <1% from 300-2000 nm, increasing to 1.26% above 2000 nm (Richard et al., 2019).

Specifically, the $\boldsymbol{\alpha}$ spectrum in our study, from 200 to 2365 nm, is an average of daily TSIS-1 SIM irradiance observations from 1-7 December 2019, which is a time period that coincides with the solar activity minimum between solar cycles 24 and 25 based on a 13-month smoothing of the sunspot number (https://www.swpc.noaa.gov/news/solar-prediction-scientists-announce-solar-cycle-25). We extend this averaged spectrum from 2365 to 2730 nm with averaged CSIM observations from April to September, 2019. The CSIM uncertainty includes the error contribution from neglecting solar variability at these infrared wavelengths. A wavelength-independent offset factor of 0.9921 ensures the CSIM irradiance portion of the $\boldsymbol{\alpha}$ spectrum (i.e. $\geq$ 2365 nm) matches TSIS-1 SIM irradiance at 2365 nm. This 0.8% offset is within the 1.26% CSIM measurement uncertainty.

3.2 High Spectral Resolution ($\boldsymbol{\beta}$) Datasets

The $\boldsymbol{\beta}$ datasets are the Air Force Geophysical Laboratory (AFGL) ultraviolet solar irradiance balloon observations, the ground-based Kitt Peak National Observatory (KPNO) solar transmittance atlas, the ground-based Quality Assurance of Spectral Ultraviolet Measurements In Europe (QASUME) Fourier transform spectrometer (QASUMEFTS) solar irradiance observations, and the semi-empirical Solar Pseudo-Transmittance Spectrum (SPTS) atlas. Brief descriptions of each are given below and key details can be found in the respective references.

Grating spectrometer observations of the Sun's ultraviolet irradiance from high-altitude balloons dating to the 1970's and 1980's by the Air Force Geophysical Laboratory (AFGL) (Hall & Anderson, 1991) are the only solar spectral irradiance dataset available to date between 200 nm and 310 nm with a spectral resolution of 0.01 nm or better. Corrections for atmospheric ozone absorption attenuation were applied to the data. The spectral and sampling resolution of the AFGL irradiance dataset are 0.01 nm and the radiometric uncertainty is typically 5-10%, but can reach 25% near 200 nm.

Additional high resolution data are solar transmittances between 300 and 1000 nm (Kurucz, 2005) derived from at the Kitt Peak National Observatory (KPNO) ground-based Fourier transform spectroradiometer (FTS) observations between 296 and 1300 nm at ~0.001 nm resolution (Kurucz et al., 1984). The conversion from FTS observations to a transmittance was achieved by an iterative, multi-step process (Kurucz, 2005). The steps involved removing continuum atmospheric absorption features based on a model followed by the estimation and removal of the solar continuum with subjective fits of the FTS observations to a simulated solar spectrum. Sharp telluric spectral features, attributed to molecules in Earth's atmosphere, were identified with the HITRAN database (Rothman et al., 2005) and removed. The KPNO residual irradiance wavelength scale accuracy, reassessed for this study, is found to be better than 3.2×10^{-4} nm above 305 nm and better than 3.0×10^{-3} nm at shorter wavelengths**,** unchanged from that reported in Chance and Kurucz (2010).

An additional source is the high-resolution extraterrestrial solar irradiance spectrum measured by an FTS between 305 nm and 380 nm from a high-altitude, ground location during the Quality Assurance of Ultraviolet Measurements In Europe (QASUMEFTS) campaign. The measured spectrum was extended down to 300 nm and up to 500 nm with the KPNO atlas (Gröbner et al., 2017). The extraterrestrial solar spectrum was derived from QASUME observations by the Langley plot technique (e.g., Arvesen et al., 1969). The FTS observations were adjusted to the absolute irradiance scale of a lower-resolution, reference spectroradiometer with accuracy traceable to the primary spectral irradiance standard of the Physikalisch Technische Bundesanstalt (PTB) laboratory in Germany. QASUMEFTS radiometric uncertainty reaches 4% at wavelengths lower than 310 nm and 2% between 310 and 500 nm. The spectral resolution of QASUMEFTS is better than 0.025 nm and uncertainty in the wavelength-scale is 0.01 nm or better.

Version 2016 of the 'disk-integrated' Solar Pseudo-Transmittance Spectrum (SPTS) (Toon, 2014) contains the transmittance from 40,000 solar absorption lines spanning 600-26316 cm^{-1} (380-16600 nm), sampled every 0.01 cm^{-1}. It is an empirically-generated dataset, where telluric line contributions to the observed spectra from multiple FTS instruments (both ground- and space-based) are identified with the HITRAN database and iteratively removed. Measured KPNO spectra are the predominant observation source in the SPTS database, supplemented with observations from high-altitude balloons and satellites (Toon, 2013).

We adopt a vacuum wavelength scale for the HSRS. Conversions from air-to-vacuum wavelengths were applied to the AFGL and QASUMEFTS datasets using Edlén's (1966) standard air dispersion formula.

4 Results

In this section, we present the TSIS-1 Hybrid Solar Reference Spectrum (HSRS) and make comparisons to independent datasets.

4.1 *Q* factor

When the spectral ratio method is used to adjust an *irradiance* dataset, the *Q* factor is unitless and represents a magnitude adjustment to the radiometric calibration of the original dataset. However, when the method is applied to adjust a *solar transmittance* dataset, the *Q* factor has units of solar spectral irradiance (Watts/m^2/nm) and approximates the continuum of the Sun's spectral irradiance when devoid of absorption and emission features. In either case, the *Q* factor adjusts broad, continuum features while leaving fine spectral features undisturbed.

Figure 2 shows the *Q* factors used to produce the HSRS at the high accuracy $\boldsymbol{\alpha}$ irradiance scale. The adjustments are smaller than 25% for AFGL and 2.5% for QASUMEFTS datasets, which falls within their respective reported radiometric uncertainties. The adjustments for the

KPNO and SPTS solar transmittance datasets have the expected spectral shape of the Sun's continuum.

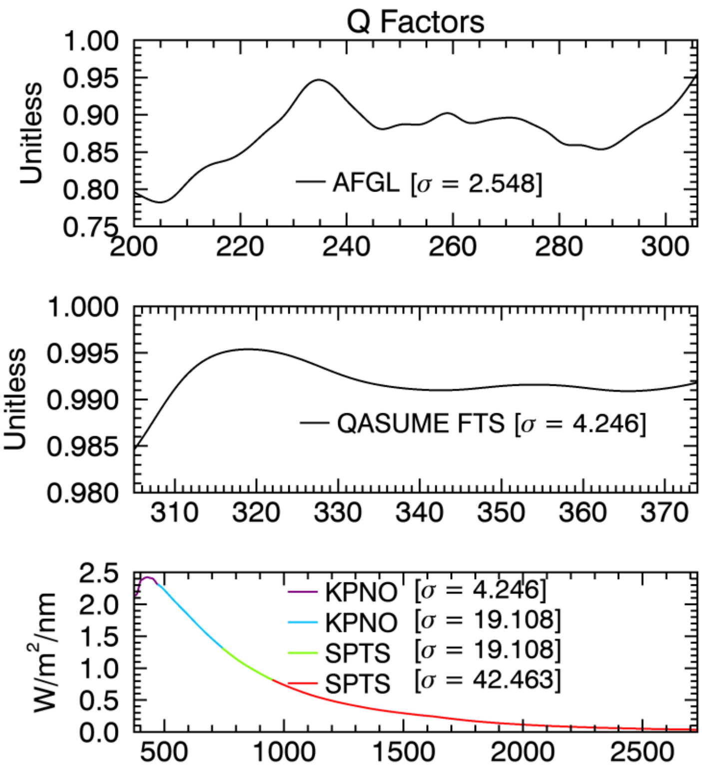

Figure 2. The wavelength-dependent *Q* factors used to adjust the AFGL, QASUMEFTS, KPNO and SPTS datasets to the absolute radiometric scale of the TSIS-1 SIM and CSIM instruments using the Gaussian convolution filters (see Eq. 2) of the specified standard deviation (σ) reported in the legends.

Applying the *Q* factors to the high resolution $\boldsymbol{\beta}$ datasets forms the TSIS-1 HSRS shown in Figure 3 (top; black) at 0.01 to ~0.001 nm spectral resolution and spanning 202 to 2730 nm. We also produce four variants of the HSRS by applying Gaussian convolution kernels in order to standardize the reference spectrum to fixed, lower spectral resolutions; two of these variants are also shown in Figure 3. The integrated solar spectral irradiance of the HSRS and the HSRS variants matches the integral of the $\boldsymbol{\alpha}$ spectrum between 202 and 2730 nm (1324.94 W m^{-2}) to within 0.2%. We produce an additional variant of the HSRS dataset (not shown) over the spectral range 202 to 500 nm with variable Gaussian convolution kernels that approximate the spectral resolution, but not the true spectral shape, of the SORCE Solar-Stellar Irradiance Comparison Experiment (SOLSTICE) (McClintock et al., 2005) and the Aura Ozone Monitoring Instrument (OMI) (Levelt et al., 2006). This final variant has utility for developing new, higher resolution, solar irradiance variability models (Lean et al., 2020). The HSRS and its variants, summarized in Table 1, are reported on fixed wavelength grids of at least 4 points per resolution element.

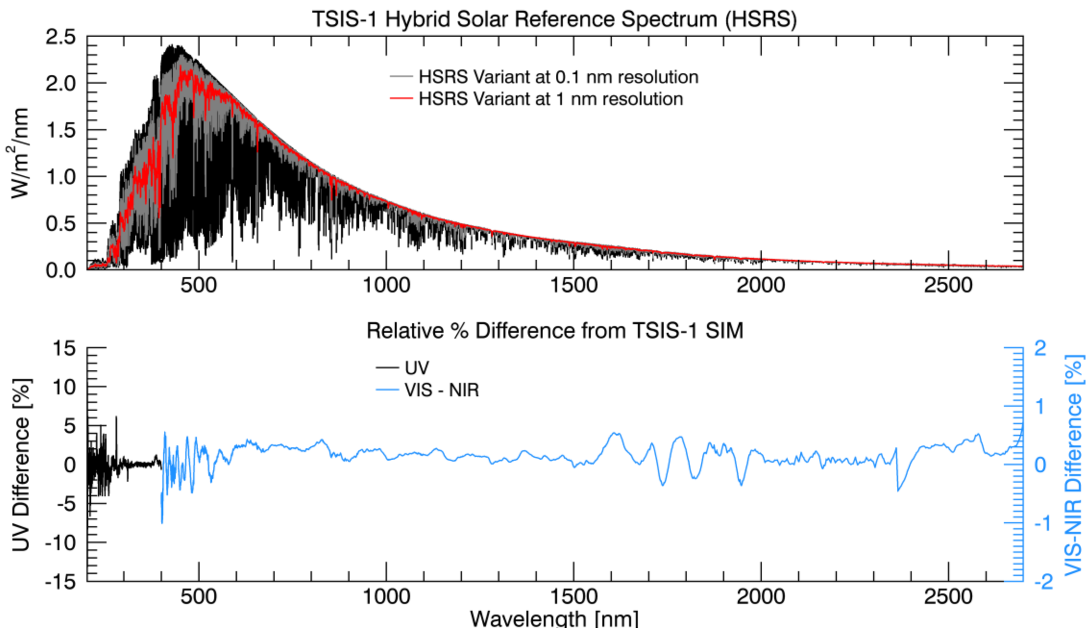

Figure 3. (top) The TSIS-1 Hybrid Solar Reference Spectrum (black) and two HSRS variants at lower resolution. (bottom) The relative percent difference of the HSRS from the high accuracy (α) spectrum, computed identically as in Figure 1, with separate percent difference y-axis scales for the ultraviolet (UV; < 400 nm) and visible-to-near-infrared (VIS-NIR; >400 nm) portions of the spectrum.

Figure 3 (bottom) shows the relative percent difference between the HSRS and the high accuracy $\boldsymbol{\alpha}$ spectrum. The HSRS has been convolved with the measured TSIS-1 SIM and CSIM instrument line shapes prior to taking the difference. Near-identical results (not shown) are obtained when computing the relative difference for the HSRS variants.

Table 1. A summary of the specifications for the TSIS-1 Hybrid Solar Reference Spectrum (HSRS) dataset and its variants. Identified for each HSRS spectrum is the spectral range covered by the high resolution β datasets, the spectral and sampling resolutions, and the uncertainty. For the purposes of this study, spectral resolution of the HSRS variants is defined by the full-width half-maximum value of the Gaussian convolution kernel.

File Name	High resolution Datasets and Wavelength Coverage (nm)	Spectral Resolution	Sampling resolution	Uncertainty (%)
TSIS-1 HSRS	AFGL: 202 - 306.5 QASUMEFTS: 305.5 - 373.6 KPNO: 373.5 - 745 SPTS: 743 - 2730	Varies; equal to that of the original high resolution, $\boldsymbol{\beta}$, datasets	0.001 nm	<400 nm = 1.3 400-2365 nm = 0.3 >2365 nm = 1.3
TSIS-1 HSRS 'p005nm'	Same as TSIS-1 HSRS	0.025 nm (below 374 nm) 0.005 nm (above 374 nm)	0.001 nm	Same as above
TSIS-1 HSRS 'p025nm'	Same as TSIS-1 HSRS	0.025 nm	0.005 nm	Same as above

TSIS-1 HSRS ‘p1nm’	Same as TSIS-1 HSRS	0.1 nm	0.025 nm	Same as above
TSIS-1 HSRS ‘1nm’	Same as TSIS-1 HSRS	1 nm	0.2 nm	Same as above
TSIS-1 HSRS ‘SOL-OMI’	AFGL: 202 - 309.8 QASUMEFTS: 306.4 - 373.5 KPNO: 373.3 - 500	0.048 nm (below 310 nm) 0.42 nm (310 to 360 nm) 0.62-0.64 nm (360 to 500 nm)	0.025 nm	<400 nm = 1.3 400-500 nm = 0.3

4.2 Uncertainties

The total TSIS-1 HSRS uncertainty (Table 1; far right) is the root-sum-square of the following error sources: the uncertainties of the TSIS-1 SIM and CSIM measurements that comprise the $\boldsymbol{\alpha}$ spectrum and the methodology accuracy. We estimate this second component from the 1-$\boldsymbol{\sigma}$ standard deviation of the relative percent difference of the HSRS and the $\boldsymbol{\alpha}$ spectrum (Figure 3; bottom). The HSRS uncertainty is equivalent to 0.3% over most of the spectrum, increasing to 1.3% below 400 nm and above 2365 nm. It reflects the uncertainty of the HSRS *for the same spectral resolution as the TSIS-1 and the CSIM instruments*. At very high spectral resolution, the relative differences in individual lines from different solar line databases can reach several tens of percent (not shown).

4.3 Comparison to Other Datasets

The combined results of Figures 1 and 3 establish that the HSRS differs from the ATLAS-3 and LASP WHI solar reference spectra on the order of several percent between 500 nm and 1300 nm, increasing to 8-10% for wavelengths outside of that range. The HSRS differs from the SOLAR-ISS reference spectrum by +3.3% (~+0.06 W m^{-2}) near the peak of the solar spectrum at 520 nm and by -2 to -4% (-0.01 to -0.03 W m^{-2}) between 800 nm and 1400 nm. In the ultraviolet, differences between the HSRS and SOLAR-ISS can approach 10%. Above 1500 nm, however, the agreement is generally within 2%.

In Figure 4, we show a comparison of the HSRS to high-resolution TANSO Fourier Transform Spectrometer (TANSO-FTS) observations obtained during solar calibration scans of the Greenhouse Gases Observing Satellite (GOSAT) mission (Kuze et al., 2009). For the comparison, the HSRS resolution has been reduced to match that of the TANSO-FTS instrument. We also apply adjustments to the TANSO-FTS data. First, we correct the wavelength scale for the Doppler shift that occurs with changing spacecraft velocity. Second, we convert the s- and p-polarized solar radiance to solar irradiance under the assumption of a perfect solar diffuser plate. Third, we average the Doppler-corrected, s- and p-polarized irradiance to get the unpolarized solar irradiance spectrum. Finally, we adjust the irradiance scale to match that of the HSRS using the spectral ratio method described in Section 2. The resulting 1-$\boldsymbol{\sigma}$ standard deviation of the HSRS and TANSO-FTS relative percent difference is smaller than 0.4% in all bands (not shown), demonstrating robust HSRS solar line positions and depths in these wavelength ranges.

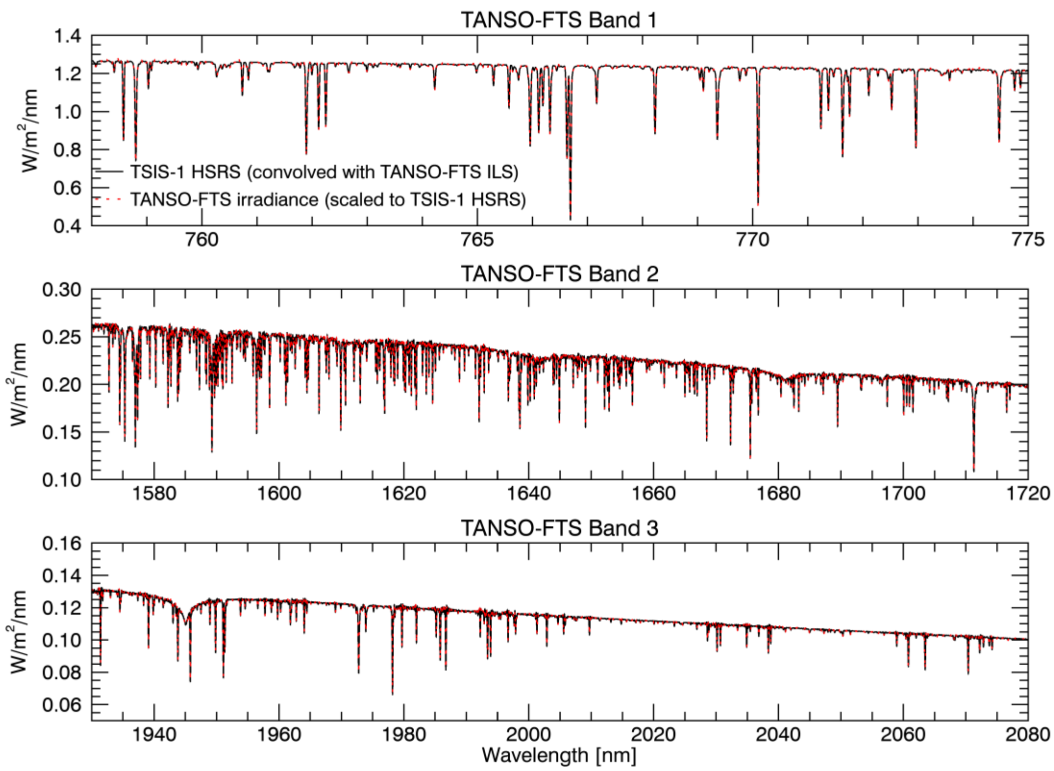

Figure 4. A comparison of the TSIS-1 HSRS to a GOSAT TANSO-FTS solar irradiance spectrum derived from solar radiances measured in three bands during calibration scans (see text).

5 Conclusions

The TSIS-1 Hybrid Solar Reference Spectrum (HSRS) is a new solar irradiance reference spectrum developed by normalizing high spectral resolution solar line data to the absolute irradiance scale of the TSIS-1 SIM and CSIM observations at solar minimum between solar cycles 24 and 25. TSIS-1 SIM and CSIM observe the Sun's irradiance spectrum at higher accuracy than attained by predecessor instruments and, notably, show the near-infrared solar spectrum is reduced in magnitude by up to 8-10% relative to some other often-used solar reference spectra. Therefore, the HSRS provides an important new constraint for science analyses in a broad array of fields.

The HSRS spans 202 to 2730 nm, encompassing an integrated energy that exceeds 97% of the total solar irradiance. The HSRS accuracy is 0.3% to 1.3% and the spectral resolution is 0.01 nm to ~0.001 nm. Variants of the HSRS are also provided for lower, fixed spectral resolutions.

Acknowledgments, Samples, and Data

The TSIS-1 HSRS is available from https://lasp.colorado.edu/lisird/. The authors extend their gratitude to the teams responsible for the development and maintenance of the AFGL, QASUMEFTS, KPNO, and JPL SPTS databases. Additionally, the authors extend their gratitude to F. Kataoka and A. Kuze for provision and assistance with the GOSAT solar calibration radiance data, to M. Snow for provision of the SORCE SOLSTICE instrument line shape information, and to S. Marchenko for the Aura OMI instrument line shape information. OC, ER, DH, PP, and TW are grateful for the support of the NASA TSIS-1 project (80GSFC18C0056) and NASA's Solar Irradiance Science Team (80NSSC18K1304) in performing this analysis. Authors at the Harvard-Smithsonian Center for Astrophysics thank NASA for ongoing support for development of satellite measurements of the Earth's atmosphere.

References

Apell, J. N., & McNeill, K. (2019), Updated and validated solar irradiance reference spectra for estimating environmental photodegradation rates. *Environ. Sci.: Processes Impacts*, 21, 2153-2153.

Arvesen, J. C., Griffin, R. N., & Pearson, B. D. (1969), Determination of Extraterrestrial Solar Spectral Irradiance from a Research Aircraft. *Appl. Opt*. 8, 2215-2232.

Berk, A., Conforti, P., Kennett, R., Perkins, T., Hawes, F., & van den Bosch. J., (2014), MODTRAN6: a major upgrade of the MODTRAN radiative transfer code. *Proc. SPIE 9088, Algorithms and Technologies for Multispectral, Hyperspectral, and Ultraspectral Imagery XX*, 90880H. doi:10.1117/12.2050433

Chance, K., & Kurucz, R. L. (2010), An improved high-resolution solar reference spectrum for earth's atmosphere measurements in the ultraviolet, visible, and near infrared. *J. of Quant. Spec. and Rad. Tran*., 111(9), 1289-1295.

Coddington, O., Lean, J. L., Pilewskie, P., Snow, M., & Lindholm, D. (2016), A Solar Irradiance Climate Data Record. *Bull. Amer. Meteor. Soc.*, 97, 1265–1282. https://doi.org/10.1175/BAMS-D-14-00265.1

Dobber, M., Voors, R., Dirksen, R., Kleipool, Q., & Levelt, P. (2008), The High-Resolution Solar Reference Spectrum between 250 and 550 nm and its Application to Measurements with the Ozone Monitoring Instrument. *Sol. Phys.*, 249**,** 281–291. https://doi.org/10.1007/s11207-008-9187-7

Edlén, B. (1966), The Refractive Index of Air, *Metrologia*, 2(2).

Elsey, J., Coleman, M.D., Gardiner, T., & Shine, K.P. (2017), Can measurements of the near-infrared solar spectral irradiance be reconciled? A new ground-based assessment between 4,000 and 10,000 cm−110,000 cm−1. *Geophys. Res. Lett.* 44(19), 10071.

Gröbner, J., Kröger, I., Egli, L., Hülsen, G., Riechelmann, S., & Sperfeld, P. (2017), The high-resolution extraterrestrial solar spectrum (QASUMEFTS) determined from ground-based solar irradiance measurements. *Atmos. Meas. Tech*., 10, 3375–3383. https://doi.org/10.5194/amt-10-3375-2017

Gueymard, C. A. (2003), The sun's total and spectral irradiance for solar energy applications and solar radiation models. *Sol. Energy*, 76, 423–453.

Hall, L. A., & Anderson, G. P. (1991), High resolution solar spectrum between 200 and 3100 A. *J. Geophys. Res*., 12927-12931. https://doi.org/10.1029/91JD01111

Harder J., Lawrence G., Fontenla J., Rottman G., & Woods T. (2005), *The Spectral Irradiance Monitor: Scientific Requirements, Instrument Design, and Operation Modes*. In: Rottman G., Woods T., George V. (eds) The Solar Radiation and Climate Experiment (SORCE). Springer, New York, NY. https://doi.org/10.1007/0-387-37625-9_9

Harder, J.W., Thuillier, G., Richard, E.C., Brown, S. W., Lykke, K. R., Snow, M., et al. (2010), The SORCE SIM Solar Spectrum: Comparison with Recent Observations. *Sol. Phys.*, 263**,** 3–24. https://doi.org/10.1007/s11207-010-9555-y

Hilbig, T., Weber, M., Bramstedt, K., Noël, S., Burrows, J. P., Krijger, J. M., et al. (2018), The New SCIAMACHY Reference Solar Spectral Irradiance and Its Validation. *Sol. Phys.*, 293**,** 121. https://doi.org/10.1007/s11207-018-1339-9

Kang, M. Ahn, M-H., Liu, X., Chance, K., Sun, K., & Kim, J. (2017), High Resolution Reference Solar Spectrum for TEMPO/GEMS and beyond. *GSICS annual meeting, 2017 Annual GSICS Joint Working Groups Meeting*, 20 – 24 March 2017, Madison, USA Available online from http://gsics.atmos.umd.edu/pub/Development/20170320/4g_Mina_High_resolution_reference_solar_spectrum_for_%20GEMS_and%20_TEMPO.pdf [Last accessed July 28, 2020].

Kang, M., Ahn, M.-H., Liu, X., Jeong, U., & Kim, J. (2020), Spectral Calibration Algorithm for the Geostationary Environment Monitoring Spectrometer (GEMS). *Remote Sens.*, 12, 2846.

Kieffer, H. H., & Stone, T. C. (2005), The spectral irradiance of the moon. *Astron. J.*, 129, 2887-2901.

Kunze, M., Kruschke, T., Langematz, U., Sinnhuber, M., Reddmann, T., & and Matthes, K. (2020), Quantifying uncertainties of climate signals in chemistry climate models related to the 11-year solar cycle – Part 1: Annual mean response in heating rates, temperature, and ozone. *Atmos. Chem. and Physics*, 20(11). 6991-7019. 10.5194/acp-20-6991-2020.

Kurucz, R. (2005), High Resolution Irradiance Spectrum from 300 to 1000 nm. *AFRL Transmission Meeting*, 15-16 June 2005, Lexington, Mass. Available online from https://arxiv.org/pdf/astro-ph/0605029.pdf [last accessed July 25, 2020].

Kurucz, R.L., & Bell, B. (1995), *Atomic Line List*, Smithsonian Astrophys. Obs., Cambridge, Mass.

Kurucz, R.L., Furenlid, I., Brault, J., & Testerman. L. (1984), *Solar Flux Atlas from 296 to 1300nm*. National Solar Observatory, Sunspot, New Mexico, 240 pp.

Kuze, A., Suto, H., Nakajima, M., & Hamazaki, T. (2009), Thermal and near infrared sensor for carbon observation Fourier-transform spectrometer on the Greenhouse Gases Observing Satellite for greenhouse gases monitoring. *Appl. Opt.*, 48, 6716-6733.

Lean, J. L., Coddington, O., Marchenko, S. V., Machol, J., DeLand, M. T., & Kopp, G. (2020), Solar irradiance variability: Modeling the measurements. *Earth and Space Science*, 7, e2019EA000645. https://doi.org/10.1029/2019EA000645

Levelt, P. F., van den Oord, G. H. J., Dobber, M. R., Malkki, A., Visser, H., de Vries, J., et al. (2006), The ozone monitoring instrument. *IEEE Transactions on Geoscience and Remote Sensing*, 44(5), 1093-1101. Doi:10.1109/TGRS.2006.872333.

Mauceri, S., Richard, E., Pilewskie, P., Harber, D., Coddington, O., Béland, S., et al. (2020), Degradation Correction of TSIS SIM, *Solar Physics*, accepted.

Mcclintock, W.E., Rottman, G.J. & Woods, T.N. (2005), Solar–Stellar Irradiance Comparison Experiment II (Solstice II): Instrument Concept and Design. *Sol. Phys.*, 230, 225–258. https://doi.org/10.1007/s11207-005-7432-x

Meftah, M., Damé, L., Bolsée, D., Pereira, N., Snow, M., Weber, M., et al. (2020), A New Version of the SOLAR-ISS Spectrum Covering the 165 – 3000 nm Spectral Region. *Sol. Phys.*, 295**(**14). https://doi.org/10.1007/s11207-019-1571-y

Pan, C., & Flynn, L. E. (2015), Solar observation of Ozone Mapping and Profiler Suite nadir system during the first 3 years of on-orbit operation. *J. of Applied Remote Sensing*, 9(1). https://doi.org/10.1117/1.JRS.9.094095

Richard, E., Harber, D., Drake, G., Rutkowski, J., Castleman, Z., Smith, M., et al. (2019), Compact spectral irradiance monitor flight demonstration mission. *Proc. SPIE 11131, CubeSats and SmallSats for Remote Sensing III*, 1113105. doi:10.1117/12.2531268.

Richard, E., Harber, D., Coddington, O., Drake, G., Rutkowski, J., Triplett, M., et al. (2020), SI-traceable Spectral Irradiance Radiometric Characterization and Absolute Calibration of the TSIS-1 Spectral Irradiance Monitor (SIM). *Remote Sens.***,** 12(11), 1818. https://doi.org/10.3390/rs12111818

Rothman, L. S., Jacquemart, D., Barbe, A., Chris Benner, D., Birk, M, Brown, L. R., et al. (2005), The HITRAN 2004 molecular spectroscopic database. *JQSRT*, 96, 139-204

Stephens, G., Freeman, A., Richard, E., Pilewskie, P., Larkin, P., Chew, C., et al. (2020), The Emerging Technological Revolution in Earth Observations. *Bull. Amer. Met. Soc.*, 101(3), E274-E285. doi:10.1175/BAMS-D-19-0146.1

Thuillier, G., Floyd, L., Woods, T.N., Cebula, R., Hilsenrath, E., Hersé, M., & Labs, D. (2004), Solar irradiance reference spectra. In: Pap, J.M., Fox, P., Fröhlich, C., Hudson, H.S., Kuhn, J., McCormack, J., North, G., Sprigg, W., Wu, S.T. (eds.) *Geophys. Monogr.* 141, 171.

Tomlin, N. A.,Yung, C. S., Castleman, Z., Denoual, A. M., Drake, G., Farber, N., et al. (2020), Overview of microfabricated bolometers with vertically aligned carbon nanotube absorbers. *AIP Advances* 10, 055010. doi: 10.1063/5.0004025

Toon, G. C. (2014), *Solar line list for GGG2014*. TCCON data archive, hosted by the Carbon Dioxide Information Analysis Center, Oak Ridge National Laboratory, Oak Ridge, Tennessee, U.S.A., doi:10. 14291/tccon.ggg2014.solar.R0/1221658, 2014. Available online from https://mark4sun.jpl.nasa.gov/toon/solar/solar_spectrum.html [last accessed July 25, 2020].

Toon, G. C. (2013), The Solar Spectrum: an Atmospheric Remote Sensing Perspective. Noble Seminar, University of Toronto, 21 Oct. 2013, Toronto, Canada. Available online from https://mark4sun.jpl.nasa.gov/report/UT_seminar_Solar_Spectrum_Toon.pdf

Werdell, P.J., Behrenfeld, M.J., Bontempi, P.S., Boss, E., Cairns, B., Davis, G.T., et al. (2019), The Plankton, Aerosol, Cloud, ocean Ecosystem (PACE) mission: Status, science, advances. *Bull. Amer. Meteor. Soc.*, 100(9), 1775-1794. doi:10.1175/BAMS-D-18-0056.1

Wielicki, B. A., Young, D. A., Mylnczak, M. G., Leroy, S., Corliss, J. Anderson, J. G., et al. (2013), Achieving Climate Change Absolute Accuracy in Orbit. *Bull. Amer. Meteor. Soc.*, 94, 1519–1539. https://doi.org/10.1175/BAMS-D-12-00149.1.

Woods, T.N., Chamberlin, P.C., Harder, J.W., Hock, R.A., Snow, M., Eparvier, F.G., et al. (2009), Solar Irradiance Reference Spectra (SIRS) for the 2008 Whole Heliosphere Interval (WHI). *Geophys. Res. Lett.* 36(1), L01101.